A study on crown interception with four dominant tree species: a direct measurement

Xiang Li, Jianzhi Niu, Linus Zhang, Qingfu Xiao, Gregory E. McPherson, Natalie van Doorn, Xinxiao Yu, Baoyuan Xie, Salli Dymond, Jiao Li, Chen Meng and Ziteng Luo

ABSTRACT

An experiment was conducted to concentrate on the rainfall interception process of individual trees for four common species in Beijing, China, which included needle species (*Platycladus orientalis* and *Pinus tabulaeformis*) and broadleaf species (*Quercus variabilis* and *Acer truncatum*). Two types of interception storages, the maximum (C_{max}) and the minimum interception storage (C_{min}), were examined at four simulated rainfall intensities (from 11.7 to 78.5 mm h^{-1}). Results showed that an average of 91% of C_{max} for all the species was intercepted during the first 10 minutes of rainfall, while 45% of C_{max} drained off after rainfall cessation. Leaf area index (LAI) and leaf area (LA) were significantly correlated ($p < 0.05$) with C_{max} and C_{min}, while such significant correlations were not found between rainfall intensity and C_{max} and C_{min}. Average C_{max} and C_{min} across all the species corresponded to 3 and 1% of gross rainfall. Mean C_{max} and C_{min} of the needle species were 3.0 and 1.8 times larger than that for the broadleaf ones. Results revealed that interception was a dynamic process which encompassed three phases. In addition, LAI and LA were valid predictors of interception in small trees, and deserve further test in forest stands.

Key words | interception process, interception storage, leaf area, leaf area index, rainfall intensity, tree species

Xiang Li
Jianzhi Niu (corresponding author)
Xinxiao Yu
Baoyuan Xie
Jiao Li
Chen Meng
Ziteng Luo
Key Laboratory of Soil and Water Conservation and
   Desertification Combating of Education
   Ministry,
Beijing Forestry University,
Beijing 100083, China
E-mail: nexk@bjfu.edu.cn

Linus Zhang
Department of Water Resources Engineering,
Lund University,
Lund 221 00, Sweden

Qingfu Xiao
Department of Land, Air and Water Resources,
University of California,
Davis, CA 95618, USA

Gregory E. McPherson
Salli Dymond
USDA Forest Service,
Pacific Southwest Research Station,
Davis, CA 95618, USA

Natalie van Doorn
USDA Forest Service,
Pacific Southwest Research Station,
Albany, CA 94710, USA

INTRODUCTION

Rainfall interception refers to the proportion of rainwater that is temporarily intercepted and stored on vegetation surfaces, and subsequently evaporates to the atmosphere or drains to the ground as throughfall (*TF*) or stemflow (*SF*) (Muzylo *et al.* 2009). Acting as a rainfall mitigating buffer, interception usually accounts for 10–60% gross precipitation (Llorens & Domingo 2007; Gerrits *et al.* 2010), and also is widely accepted to affect the subsequent hydrologic processes, such as evaporation, transpiration, infiltration, and surface runoff (Savenije 2004; Janeau *et al.* 2015).

Interception has usually been studied on three scales: the single branch level (with foliage) (Keim *et al.* 2006; Xiao & McPherson 2015), the individual tree level (Asadian & Weiler 2009; Xiao & McPherson 2011), and the forest stand level (Dietz *et al.* 2006; Safeeq & Fares 2014). In most of these studies, interception has been indirectly calculated by the difference between gross rainfall and the sum of *TF* and *SF*, indicating that only the intercepted water for evaporation has been estimated as a flux or stock. The mechanism of the interception process which includes wetting,

saturation, and post-rainfall drainage has thus far been over-looked. However, a process-based interception is critical to clarify the rainfall-mitigating and time-lagging effect during rainfall, and thereby helps to control peak flow, flood, and erosion (Keim & Skaugset 2004). Limited results from previous studies indicated that almost 30% of intercepted rainwater tended to drip off after rainfall (Aston 1979; Pitman 1989; Keim *et al.* 2006). As a result, interception would be better characterized as a dynamic process.

According to previous investigations, interception is governed by both biotic and abiotic factors (Xiao *et al.* 2000a; Gerrits & Savenije 2011). Abiotic factors such as rainfall intensity shapes the way raindrops interact with leaf and branch surfaces: Price & Carlyle-Moses (2003) and Wang *et al.* (2007) reported that high rainfall intensity reduced interception amount because it caused splashing and shaking of the crown. Keim *et al.* (2006) and Xiao & McPherson (2015) found the opposite: interception increased with rainfall intensity given that the leaves were beyond saturated. In addition, rainfall frequency as well as air temperature, wind speed, and net radiation impacts evaporation and interception (Xiao *et al.* 2000b). On the other hand, biotic factors such as leaf morphology, roughness, inclination, and hydrophobicity tended to affect interception by modifying the intercepted-rainwater pathways inside the crown (Holder 2013; Nanko *et al.* 2013). Other factors that played a role included branch inclination, surface property, and bark texture (Herwitz 1987; Levia *et al.* 2015). Crown gap fraction controls interception as it represents the proportion of free *TF* that has no contact with the crown (Rutter *et al.* 1971). Among the biotic factors, leaf area index (LAI) and leaf area (LA) have been extensively used in previous analyses (Carlyle-Moses & Gash 2011). LAI, calculated as the total LA divided by crown projection area (CPA) (Watson 1947), has been measured indirectly in forest stands based on the transmission of light mechanism (Fleischbein *et al.* 2005). However, the overlapping canopy from different trees may have resulted in an underestimation of LAI (Breda 2003). On the other hand, few studies have quantified interception on an LA basis due to the labor-intensive and destructive measurement, although it has been recognized as an accurate indicator, and easy to scale up from single trees to forest stand level in several studies (van Dijk & Bruijnzeel 2001a, 2001b).

Therefore, the objective of this research is to quantify interception on a process basis. First, we aim to depict the wetting–saturation–drainage phases in interception. Second, we examine the influence of different biotic (LAI, LA, and leaf type) and abiotic factors (rainfall intensity) on interception.

MATERIALS AND METHODS

Tree characteristics

Four common tree species in Northern China including two conifer species (*Platycladus orientalis* and *Pinus tabulaeformis*) and two broadleaf deciduous species (*Quercus variabilis* and *Acer truncatum*) were selected for this study (China Forest Editorial Committee 2001). Two four-year-old trees for each species were chosen from the field in Jiufeng National Forestry Park, Beijing, China (116 °28′E, 39 ° 34′N). The trees were then transplanted into a 2-m-diameter plastic cylinder and were transported from the field to a rainfall simulation laboratory, where several tree characteristics were measured before rainfall simulation began (Table 1). LAI was measured using an LAI-2200 Plant Canopy Analyzer (LICOR Inc., Lincoln, NE, USA). CPA was determined from photos taken from a height of 15 m above the tree, and was further analyzed using Photoshop software (Adobe System Inc., San Jose, CA, USA). No wilting phenomenon was observed before or during the experimental procedures.

Rainfall simulator

The infrequency and unpredictability of natural rainfall makes it difficult for us to study interception on a process basis. To address this challenge, a rainfall simulator was used. Over the past few decades, a wide variety of rainfall simulators have been used to conveniently and rapidly obtain diverse rainfall intensities and interception rates (Moore *et al.* 1983). In general, at least three criteria should be taken into consideration when designing a simulator (Wilson *et al.* 2014): (1) the simulated rainfall should have physical characteristics similar to natural rainfall with respect to raindrop terminal velocity and kinetic

Table 1 │ Characteristics of the experimental trees

Tree species	Height (m)	Basal diameter (cm)	Crown height (m)	Crown diameter (m)	LAI	CPA (m^2)	LA (m^2)
PO-1	1.75	1.6	1.28	0.73	2.61	0.89	2.32
PO-2	1.81	1.5	1.09	0.85	2.02	0.76	1.54
PT-1	1.52	2.4	0.96	0.94	2.35	0.99	2.33
PT-2	1.77	2.5	1.05	0.96	2.01	1.12	2.25
QV-1	1.63	2.1	1.06	0.66	1.74	1.04	1.81
QV -2	2.24	1.9	1.64	0.75	1.32	1.22	1.61
AT-1	2.12	2.2	1.55	1.12	2.05	1.48	3.03
AT -2	1.96	2.0	1.35	0.97	1.95	1.33	2.59

LAI, leaf area index; CPA, crown projected area.

PO-1 and PO-2 represent two *Platycladus orientalis* trees, PT-1 and PT-2 represent two *Pinus tabulaeformis* trees, QV-1 and QV-2 represent two *Quercus variabilis* trees, and AT-1 and AT-2 represent two *Acer truncatum* trees.

energy; (2) the simulator should produce various rainfall intensities, and can be easily moved and operated to fit the study area; and (3) the cost must be low. Based on these principles, two types of rainfall simulators have been developed: drip tank and spray nozzles. The drip tank simulator with hypodermic needles usually operates at low pressure and thereby generates light rainfall with small raindrop diameter. The raindrop kinetic energy is mainly determined by the hanging height of the simulator (Battany & Grismer 2000). In contrast, simulators with spray nozzles, working under high pressure, can provide a wide range of raindrop diameters. Also, most of the simulated raindrops can reach 90% of the kinetic energy of natural rainfall. As a result, spray nozzle simulators have been extensively used in many studies (Fister *et al.* 2012).

The spray nozzle simulator used in this study was jointly manufactured in 2006 by Beijing Jiaotong University and Beijing Normal University. A more detailed description is presented by Zhang *et al.* (2007). The simulator is composed of a water supply system with a pump (YCGT90W, Chuanji Co. Ltd, Shanghai, China), a rainfall output system including a Veejet 80150 sprinkler with three rotation nozzles (Spraying Systems Co., Wheaton, IL, USA) and a computer-control system. The simulator is able to spray water over an area of 2.2 m × 1.5 m at a height of 4.5 m. A wide range of rainfall intensities (20 to 200 mm h^{-1}) can be simulated by a combination of different nozzle sizes and swing frequencies. Simulated raindrops have a 2.3 ± 0.3 diameter and can reach terminal velocity. The simulated rainfall uniformity

is about 80%, which is in accordance with traits of natural rainfall. Since rainfall intensities over the past 50 years in Beijing have ranged from 2.6 to 80 mm h^{-1} (Zhong *et al.* 2013), a range of low to moderate simulated rainfall intensities of 11.7, 25.2, 48.4, and 78.5 mm h^{-1} were used in the experiment for 40 minutes.

Experimental procedure

The experiments were conducted at an average temperature of 25.8 °C in the laboratory from June to September, 2012. Prior to the rainfall simulation, experimental trees were positioned on an electronic weighing balance (EP-500, E&C Co. Ltd, Shanghai, China; minimum graduation: 0.1 g) and an aluminum cover was set above the balance to exclude the effect of *TF* and *SF* on rainfall interception measurements (Figure 1). The lower edge of the aluminum cover was placed on the ground surface and the gradient of the cover was 10–20° from horizontal level. This was done to accelerate *TF* flowing down to the ground through the cover rather than allow it to infiltrate into the cylinder. A plastic reverse-funnel was cohered on the tree bole to allow *SF* to drip down to the cover. As a result, cumulative rainfall interception was recorded as the change in tree weight.

To fully depict the interception process, two different interception storages were measured: the maximum interception storage (C_{max}) and the minimum interception storage (C_{min}). C_{max} is the amount of rainwater intercepted and detained by the tree crown immediately before rainfall
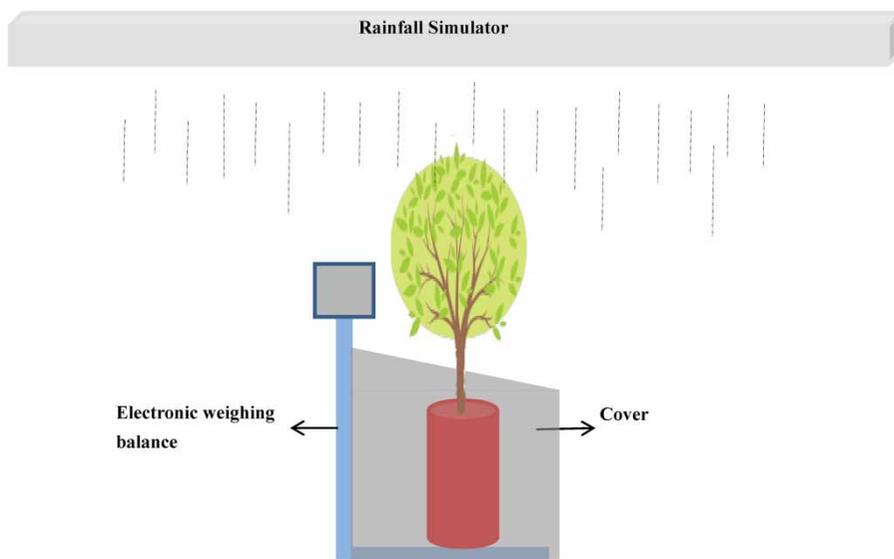
Figure 1 | Schematic diagram of the experiment.

cessation; C_{min}, taken as the amount of rainwater detained on the crown when drainage ceases after rainfall, can only be removed by evaporation (Li *et al.* 2013).

After the rainfall began, tree weight was recorded every 10 seconds in the first minute, then every 30 seconds in the next 9 minutes and every minute in the remaining 30 minutes. C_{max} was thereby calculated as the amount of intercepted water when simulated rainfall ceased. After the cessation, change in tree weight due to the leaf and branch drip was recorded every 10 seconds for the first minute, 30 seconds for the next minute, and each minute thereafter until a weight change of <0.1 g was obtained. Consequently, C_{min} was calculated as the difference in tree weight before the rainfall simulation and after the drainage process. After these primary interception experiments, tree crown was divided into three vertical layers from the bottom to the top. The leaves and branches of the bottom layer were initially removed and preserved for LA measurement. Similarly, tree traits such as crown depth, crown diameter, LAI, and CPA were remeasured. Afterwards, each tree was repositioned on the electronic weighing balance to be resubjected to the simulated rainfall. Likewise, rainfall simulation was repeated after the middle layer was removed. Total LA of broadleaves was determined by tracing the outline of every leaf, and then calculating the area using Adobe Photoshop software (Adobe System Incorporated). For

needles, LA was calculated by measuring needle length and diameter to determine the two-dimensional area, and then scaled to column, three-dimensional, and four-dimensional cones based on needle shape.

It should be mentioned that evaporation (E) was not taken into consideration in the simulation process because the amount of wind and sunlight radiation in the laboratory was considered negligible. To minimize the impact of E on the drainage process, some water was poured on the wall of the laboratory to keep a relatively stable humidity. All the examined trees were moved outside the laboratory to naturally dry the crown for 24 hours. Each test run was repeated once daily, resulting in a total of 192 rainfall events.

Statistical analysis

Pearson's correlation method was used to test whether C_{max} and C_{min} were significantly correlated with rainfall intensity, LAI, and LA. Parameters were considered to be significantly correlated when they were at or above the 95% confidence level ($p \leq 0.05$). Meanwhile, linear, polynomial, and nonlinear regressions were used to analyze the variation trend between C_{max} and C_{min} and those factors. One-way analysis of variance (ANOVA) with the Fisher LSD (least significant difference) test at $p \leq 0.05$ was used to determine if there were significant differences in C_{max}, C_{min} between the

broadleaf and coniferous species. Related data were grouped according to leaf morphology (e.g., broadleaf species were represented by *PO* and *PT*, while coniferous species were represented by *QV* and *AT*). All statistical analyses were performed using IBM SPSS Statistics 20.0 software.

RESULTS AND DISCUSSION

Rainfall interception process

The rainfall interception process by an entire tree crown over time is shown in Figure 2. Generally, the interception process included three phases: the rapid-dampening phase, the stable-saturation phase, and the drainage phase. The rapid-dampening phase usually took place in the very first 10 minutes of the rainfall, when the cumulative interception (I_C) amount accounted for 91% (STD = 8%) of C_{max}, and 175% of C_{min} regardless of species and rainfall intensities,

showing that the crown could temporarily hold water in excess of its storage capacity. As the rainfall continued for an additional 20 minutes, I_C was relatively stable because the crown was too wet (even saturated) to retain more rainwater. After rainfall, an average of 45% (STD = 6%) of C_{max} drained off for all the species, ranging from the largest drainage of 63% (STD = 5%) of C_{max} for *P. tabulaeformis*, to the lowest drainage of 15% (STD = 2%) for *A. truncatum*. The results are consistent with the drainage percentage of 10 to 70% reported in previous studies (e.g., Aston 1979; Pitman 1989; Calder *et al.* 1996a). As Xiao *et al.* (2000b) implied, in theory, there should be no drainage until the interception storage capacity is exceeded during rainfall. However, drips from the crown were observed even at the beginning of rainfall (less than 10 minutes) probably due to the steep leaf angle, leaf hydrophobicity, and downward wind created by intense rainfall, indicating that the rainfall-lagging effect of interception may have already occurred although the crown was not saturated. Given
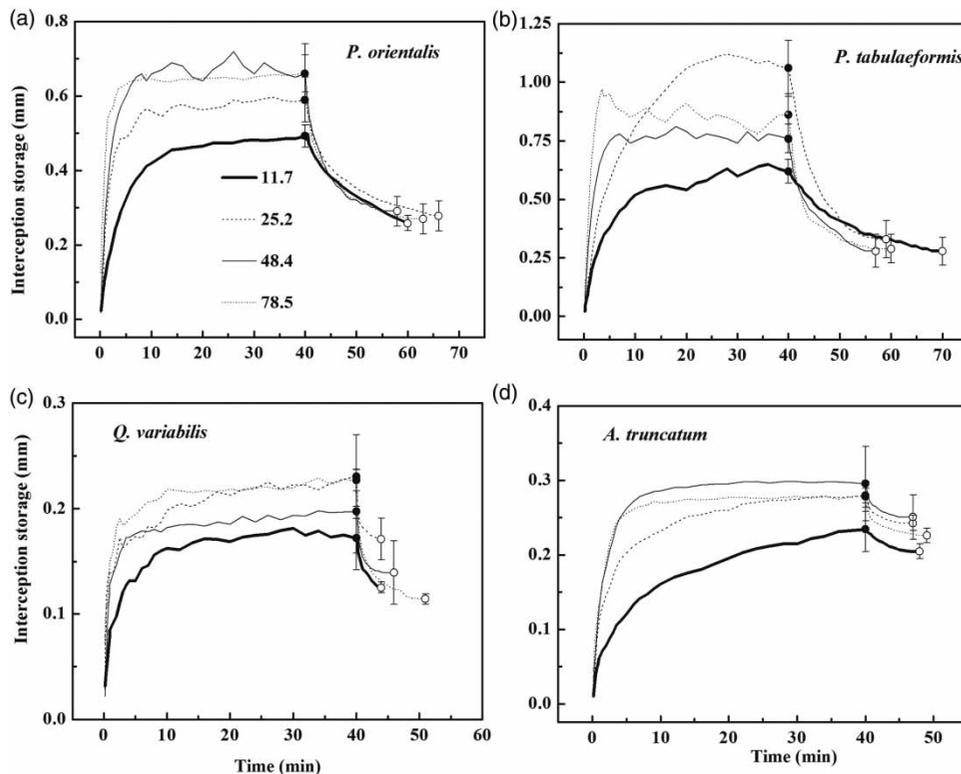

Figure 2 │ Time series of mean crown interception storage for *P. orientalis* (a), *P. tabulaeformis* (b), *Q. variabilis* (c), and *A. truncatum* (d) at four rainfall intensities. Closed symbols indicate C_{max} and open symbols indicate C_{min}. Error bars indicate STD. The C_{max} and C_{min} data are presented as mm per crown projected area (m²), the same expressions are shown in Figure 3–7.

that our experiment was conducted on a small and single tree level, we would expect that the drainage, rainfall-lagging, and peak flow delaying effect will be more considerable in mature forests, and thereby warrants further research.

Mean I_C at the first minute was 38% (STD = 18%) of the cumulative precipitation for all the species, but decreased dramatically with time in each single rainfall event thereafter (Figure 3). In the end, C_{max} and C_{min} corresponded to only 3% (STD = 2%) and 1% (STD = 1%) of the total precipitation (Figure 3). This result implied that the interception storage capacity decreased considerably with continuous wetting by rainfall.

Impact of rainfall intensity on rainfall interception

As expected, higher RIs (48.4 and 78.5 mm h^{-1}) tended to wet and saturate the crown more rapidly than lower RIs (11.7 and 25.2 mm h^{-1}) (Figure 2). However, RI showed no statistically significant correlations with C_{max} and C_{min}

(Figures 4 and 5). Further, the polynomial regression analysis revealed an increase–decrease trend of C_{max} and C_{min} with increasing RI; the largest values of C_{max} and C_{min} were not obtained at the highest RI of 78.5 mm h^{-1}. This phenomenon can result from two mechanisms. First, as we had observed, raindrops with huge kinetic energy generated by the intense rainfall (48.4 and 78.5 mm h^{-1}) splashed when hitting the leaf surface. This force, in combination with the hydrophobicity of juvenile leaves (Crockford & Richardson 1990), likely caused the interception amount to decrease. Second, the temporarily remaining droplets on leaves were partly removed by the downward wind from the intense rainfall (Dunkerley 2009).

Contradicting relationships between RI and interception storages were reported in previous studies. Price & Carlyle-Moses (2003) found that interception storage capacity when $RI < 7$ mm h^{-1} was larger than when $RI > 7$ mm h^{-1}. Calder (1996b) drew a similar conclusion when comparing the storage capacity at RIs of 36 and 45 mm h^{-1}. However, several researchers found that interception storage capacity
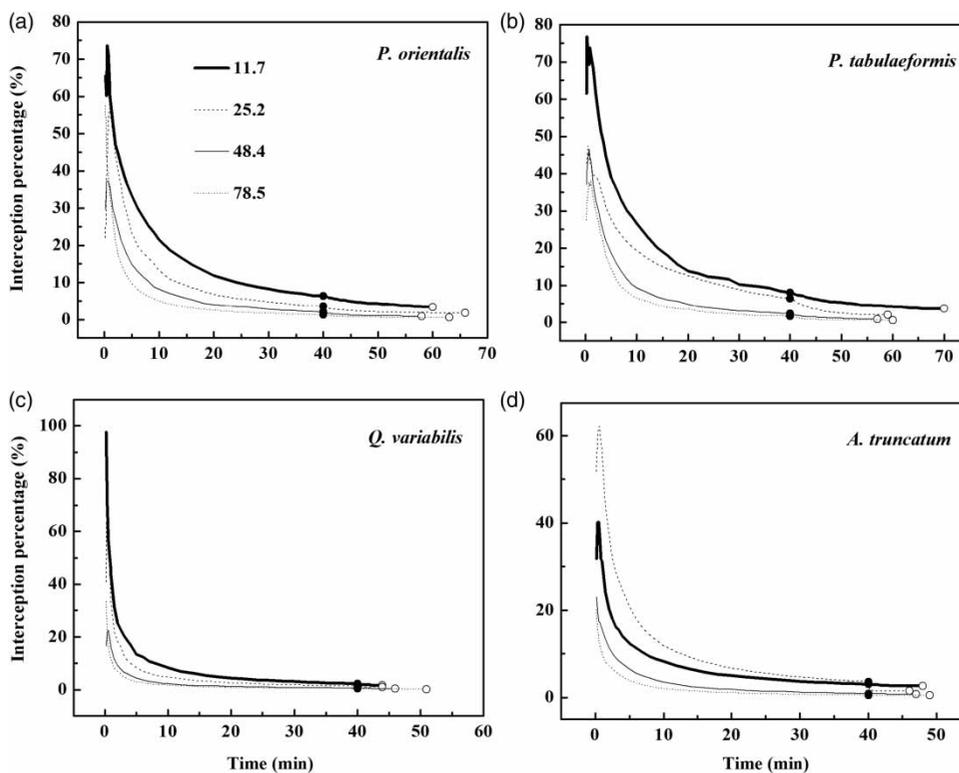

Figure 3 │ Time series of proportion of mean interception storage in accumulative precipitation for *P. orientalis* (a), *P. tabulaeformis* (b), *Q. variabilis* (c), and *A. truncatum* (d) at four rainfall intensities. Closed symbols indicate C_{max} and open symbols indicate C_{min}.
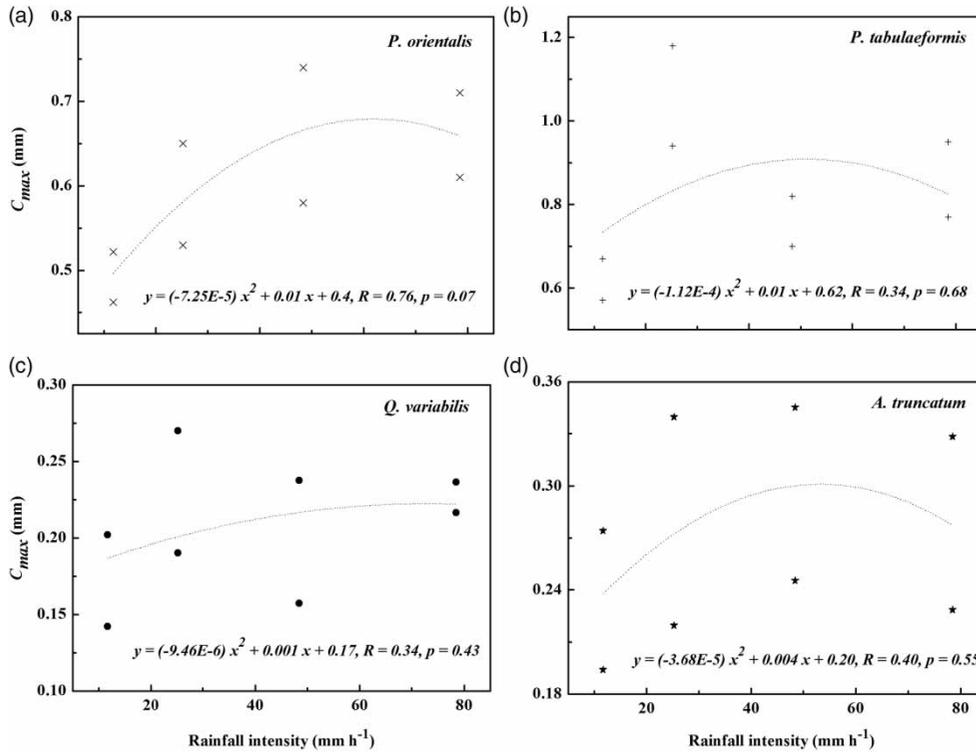
Figure 4 │ Relationships between C_{max} and rainfall intensity for all the examined trees of *P. orientalis* (a), *P. tabulaeformis* (b), *Q. variabilis* (c), and *A. truncatum* (d). N = 8.
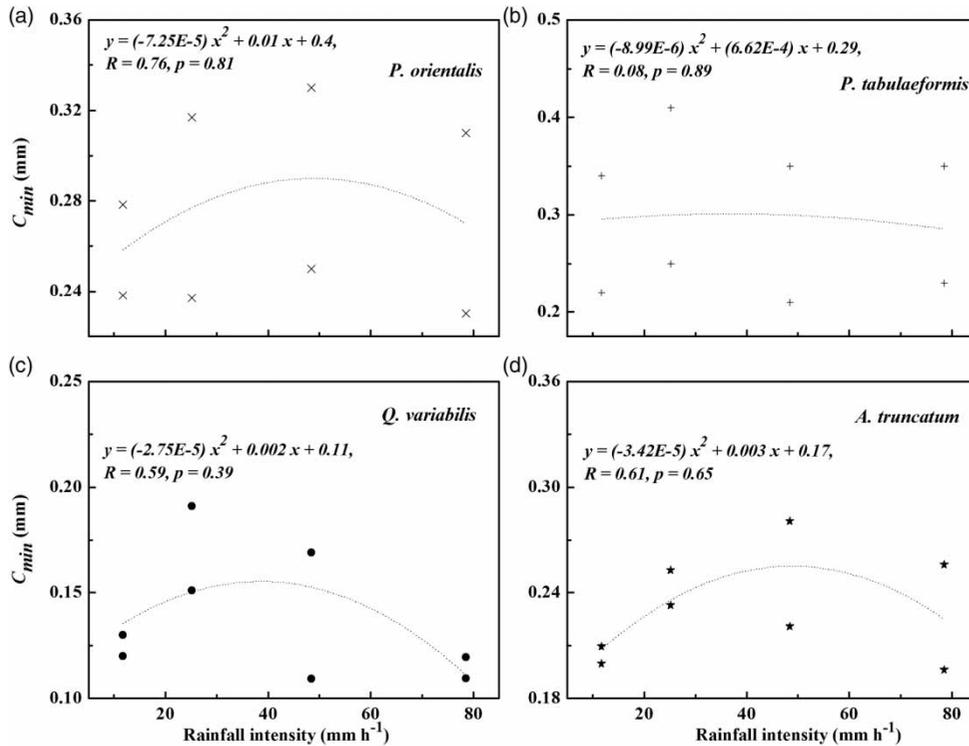

Figure 5 │ Relationships between C_{min} and rainfall intensity for *P. orientalis* (a), *P. tabulaeformis* (b), *Q. variabilis* (c), and *A. truncatum* (d). N = 8.

was larger at higher *RI*s than lower *RI*s (e.g., Aston 1979; Humbert & Najjar 1992; Keim *et al.* 2006). These outcomes also indicated that additional light rainfall experiments should be conducted to determine the threshold *RI* in the interception process.

Impact of tree characteristics on rainfall interception

The effect of crown structure parameters (particularly LAI and LA) on rainfall interception was examined. LAI showed statistically significant positive correlations ($p = 0.000$ and 0.000) with both average C_{max} and C_{min} across all species (Figure 6). Both mean C_{max} and C_{min} escalated with increasing LAI ($R > 0.9$). (*Note:* the presented mean values included C_{max} and C_{min} of the entire crown, and the remaining crowns after the first and second defoliations.) Previous studies have mainly reported two linear relationships between LAI and C_{min}: $C_{min} = \text{a} \times \text{LAI}$, where 'a' was a coefficient, ranging from 0.15 to 0.5 (Pitman 1989; Kondo *et al.* 1992; van Dijk & Bruijnzeel 2001a; Deguchi *et al.* 2006; Carlyle-Moses & Price 2007), and $C_{min} = \text{a} \times \text{LAI} + \text{b}$ (Gómez *et al.* 2001; Fleischbein *et al.* 2005), where 'a' and 'b' were coefficients. Both the polynomial model from our study and linear models from previous studies suggest that more rainwater will be intercepted with increasing LAI. However, C_{min} was greater in the linear equation

than in the polynomial equation at the same LAI. This is probably because the small and low ranges of LAI in our study (LAI = 0.57–2.61, Tables 1 and 2) compared with those in previous studies (LAI = 3–10). To be able to scale up the polynomial relationship, more tests are needed in large and mature trees spanning a wide range of LAI. Similarly, as previous studies have primarily examined single species in mature forests, additional experiments and observations are needed on various species to determine whether the linear relationships can be extrapolated to mixed species forests.

Beyond the role of leaves in intercepting rainfall, studies have recognized the importance of the role of branch and bark in interception and evaporation (Keim *et al.* 2006), particularly in leafless periods (Herbst *et al.* 2008). For instance, an index including both leaf and branch area, such as woody area index and plant area index, has been introduced in several studies (Livesley *et al.* 2014; Safeeq & Fares 2014). These expanded indices could provide stronger correlations with interception than we have observed with LA. Along those lines, it is likely that there is a positive relationship between interception rates and crown height (CH). This is because the number of overlapping leaves and branches will increase with increasing CH, which forms a multi-layer interception effect, and time delay. CH is an easily measurable metric that deserves further investigation.

Mean C_{max} and C_{min} per LA (m^2) were 0.13–0.38 and 0.09–0.13 mm across species (Table 3), which was in the range reported by Aston (1979), who found that C_{min} ranged from 0.03 to 0.18 mm for seven broadleaf and one
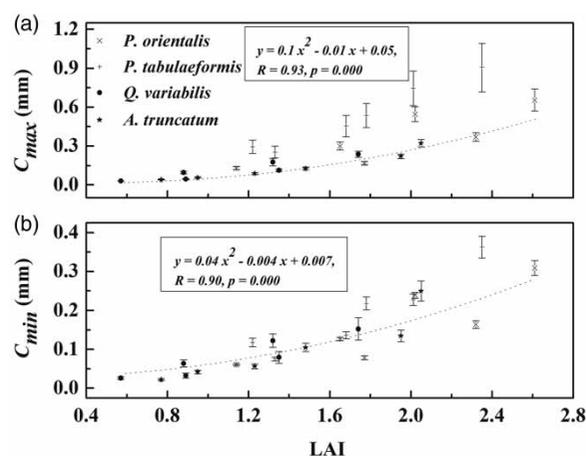

Figure 6 │ Mean C_{max} (a) and C_{min} (b) regardless of rainfall intensities in relation to leaf area index (LAI) for all the examined trees. The data included the entire crown, and remaining crowns after first and second defoliation, N = 24. Cross (×) symbols indicate *P. orientalis*, cross (+) symbols indicate *tabulaeformis*, closed circles indicate *Q. variabilis*, closed stars indicate *A. truncatum*. Error bars indicate STD.

Table 2 │ List of LAI and LA after first and second defoliation for all the experimental trees

Tree species	LAI$_{AD1}$	CPA$_{AD1}$ (m^2)	LA$_{AD1}$ (m^2)	LAI$_{AD2}$	CPA$_{AD2}$ (m^2)	LA$_{AD2}$ (m^2)
PO-1	2.32	0.58	1.35	1.77	0.33	0.58
PO-2	1.65	0.51	0.84	1.14	0.34	0.39
PT-1	1.78	0.72	1.28	1.22	0.45	0.55
PT-2	1.68	0.77	1.29	1.33	0.41	0.54
QV-1	1.35	0.76	1.03	0.89	0.45	0.40
QV -2	0.88	0.82	0.72	0.57	0.48	0.27
AT-1	1.48	1.05	1.55	0.95	0.66	0.63
AT -2	1.23	0.84	1.03	0.77	0.55	0.42

AD1 and *AD2* indicates after first and second defoliation, respectively.

Table 3 │ Values of mean C_{max} and C_{min} for each species and leaf types

Tree species	Mean C_{max} /CPA (mm)	Mean C_{min} /CPA (mm)	Mean C_{max} /LA (mm)	Mean C_{min} /LA (mm)
P. orientalis	0.60 ± 0.09	0.27 ± 0.04	0.26 ± 0.03	0.12 ± 0.01
P. tabulaeformis	0.83 ± 0.18	0.30 ± 0.07	0.38 ± 0.07	0.13 ± 0.02
Q. variabilis	0.21 ± 0.04	0.13 ± 0.03	0.13 ± 0.02	0.09 ± 0.02
A. truncatum	0.27 ± 0.03	0.19 ± 0.03	0.14 ± 0.02	0.09 ± 0.01
Needle species	0.71 ± 0.18	0.28 ± 0.06	0.32 ± 0.06	0.12 ± 0.01
Broadleaf species	0.24 ± 0.10	0.16 ± 0.05	0.13 ± 0.02	0.09 ± 0.01

CPA, crown projected area; LA, leaf area.
All the values are shown with STD.

needle species. Keim *et al.* (2006) reported that C_{max} ranged from 0.01 to 0.75 mm when testing the single branch of five broadleaf and three needle species. A larger C_{min} of 0.7 mm per LA was reported by Alavi *et al.* (2001) in a Norway spruce stand. Further, our results showed that C_{max} and C_{min} increased significantly with LA (Figure 7, $p < 0.05$, $R > 0.6$). This is mainly due to the fact that more rainwater was re-intercepted as a denser crown was formed by increasing LA. C_{max} and C_{min} showed similar linear correlation with LA in previous studies (Aston 1979; Keim *et al.* 2006), which indicates that interception can be estimated even in mixed-species forests by using the linear equation. However, the estimation should be verified in forest stand, where overlapping branches and leaves, and other factors such as

Figure 7 │ Mean C_{max} (a) and C_{min} (b) regardless of rainfall intensities in relation to leaf area (LA) for all the examined trees. The data included the entire crown, and remaining crowns after first and second defoliation, N = 24. Cross (×) symbols indicate *P. orientalis*, cross (+) symbols indicate *tabulaeformis*, closed circles indicate *Q. variabilis*, closed stars indicate *A. truncatum*. Error bars indicate STD.

branch inclination, flexibility, and above-canopy energy are different with single small trees (Pugh & Small 2013).

Leaf type also played a relevant role in determining interception. The needle crown of *P. tabulaeformis* had the highest mean C_{max} and C_{min} on both a CPA and LA basis due to its dense clusters (Table 3). This resulted in raindrops that were intercepted multiple times by the overlapped branches and needles and thereby gradually accumulated in the crown. By comparison, *Q. variabilis* with its broadleaf crown showed the lowest mean C_{max} and C_{min} because its crown was relatively open and rainwater could pass through directly. Additionally, the smooth and hairless leaves likely failed to prevent rainwater from dripping. Generally, average C_{max} and C_{min} for the needle species were 0.71 (STD = 0.18) and 0.28 (STD = 0.10) mm on a CPA basis, which was 2.96 and 1.75 times larger than that for broadleaf species regardless of rainfall intensities. Moreover, ANOVA analysis suggested that there were significant differences ($p = 0.000$ and 0.000) in C_{max} and C_{min} between the two types. These results were in line with Barbier *et al.* (2009), who in reviewing 28 articles found that needle species intercepted more rainwater than broadleaf species. Therefore, the proportion of broadleaf and needle trees (i.e., LAI ratio) in mixed forests should be taken into consideration to precisely estimate interception.
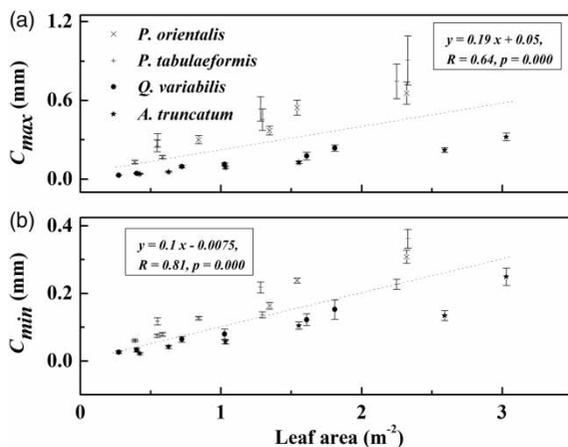
CONCLUSIONS

The present study highlighted the interception process to address some critical challenges that have seldom been

investigated. The first challenge was how to depict the rainfall interception process. Generally, the complete interception consisted of three phases, the rapid-dampening phase (0–10 minutes, 90% of C_{max} was reached), the stable-saturated phase (10–40 minutes, no evident I_C fluctuation), and the draining phase (40–70 minutes, 45% of C_{max} dripped). Almost 90% of the C_{max} amount was intercepted in the rapid-dampening phase. In the subsequent stable-saturated phase, the interception storage showed no evident fluctuation as the crown was gradually wetted and saturated. Approximately 45% of C_{max} drained off in the draining phase due to gravity. The second challenge was to evaluate the effect of rainfall characteristics and tree traits on interception. The major findings showed that LAI and LA were relevant indicators for predicting interception as they were found not only to be significantly correlated with C_{max} and C_{min}, but were adequately explained using polynomial and linear relationships. By comparison, rainfall intensity was not significantly correlated with C_{max} and C_{min}, but the co-variation trends implied that there should be a threshold rainfall intensity to influence interception. Last, needle crowns with dense branch and needle foliage distribution intercepted more rainfall water than the relatively open broadleaf crowns. Further studies are warranted to accurately quantify interception on a process basis, and establish related models with more easily measurable parameters such as CH, branch number, length, density, and inclination.

ACKNOWLEDGEMENTS

REFERENCES

Alavi, G., Jansson, P. E., Hällgren, J. E. & Bergholm, B. 2001 Interception of a dense spruce forest – performance of a simplified canopy water balance model. *Nordic Hydrol.* **32** (4/5), 265–284.

Asadian, Y. & Weiler, M. 2009 A new approach in measuring rainfall interception by urban trees in coastal British Columbia. *Water Qual. Res. J. Canada.* **44**, 16–25.

Aston, A. R. 1979 Rainfall interception by eight small trees. *J. Hydrol.* **42**, 383–396.

Barbier, S., Balandier, P. & Gosselin, F. 2009 Influence of several tree traits on rainfall partitioning in temperate and boreal forests: a review. *Ann. Forest Sci.* **66**, 602–602.

Battany, M. C. & Grismer, M. E. 2000 Development of a portable field rainfall simulator for use in hillside vineyard runoff and erosion studies. *Hydrol. Process.* **14**, 1119–1129.

Bréda, N. J. J. 2003 Ground-based measurements of leaf area index: a review of methods, instruments and current controversies. *J. Exp. Bot.* **54**, 2403–2424.

Calder, I. R., Hall, R. L., Rosier, P. T. W., Bastable, H. G. & Prasanna, K. T. 1996a Dependence of rainfall interception on drop size: 2. Experimental determination of the wetting functions and two-layer stochastic model parameters for five tropical tree species. *J. Hydrol.* **185**, 379–388.

Calder, I. R. 1996b Dependence of rainfall interception on drop size: 1. Development of the two-layer stochastic model. *J. Hydrol.* **185**, 363–378.

Carlyle-Moses, D. E. & Price, A. G. 2007 Modelling canopy interception loss from a Madrean pine-oak stand, northeastern Mexico. *Hydrol. Process.* **21**, 2572–2580.

Carlyle-Moses, D. E. & Gash, J. H. C. 2011 Rainfall interception loss by forest canopies (D. F. Levia, D. E. Carlyle-Moses & T. Tanaka, eds). *Forest Hydrology and Biogeochemistry: Synthesis of Past Research and Future Directions*. Springer Publishing, Heidelberg, Germany, pp. 407–420.

China Forest Editorial Commitee 2001 China Forest (in Chinese). China Forestry Press, Beijing, China.

Crockford, R. H. & Richardson, D. P. 1990 Partitioning of rainfall in a eucalypt forest and pine plantation in southeastern Australia: III Determination of the canopy storage capacity of a dry sclerophyll eucalypt forest. *Hydrol. Process* **4**, 157–167.

Deguchi, A., Hattori, S. & Park, H.-T. 2006 The influence of seasonal changes in canopy structure on interception loss: application of the revised Gash model. *J. Hydrol.* **318**, 80–102.

Dietz, J., Hölscher, D., Leuschner, C. & Hendrayanto, 2006 Rainfall partitioning in relation to forest structure in

differently managed montane forest stands in Central Sulawesi, Indonesia. *Forest. Ecol Manag.* **237**, 170–178.

Dunkerley, D. L. 2009 Evaporation of impact water droplets in interception processes: historical precedence of the hypothesis and a brief literature overview. *J. Hydrol.* **376**, 599–604.

Fister, W., Iserloh, T., Ries, J. B. & Schmidt, R.-G. 2012 A portable wind and rainfall simulator for in situ soil erosion measurements. *Catena* **91**, 72–84.

Fleischbein, K., Wilcke, W., Goller, R., Boy, J., Valarezo, C., Zech, W. & Knoblich, K. 2005 Rainfall interception in a lower montane forest in Ecuador: effects of canopy properties. *Hydrol. Process.* **19**, 1355–1371.

Gerrits, A. M. J. & Savenije, H. H. G. 2011 *Treatise on Water Science*. Elsevier, Oxford, UK.

Gerrits, A. M. J., Pfister, L. & Savenije, H. H. G. 2010 Spatial and temporal variability of canopy and forest floor interception in a beech forest. *Hydrol. Process.* **24**, 3011–3025.

Gómez, J. A., Giráldezb, J. V. & Fereres, E. 2001 Rainfall interception by olive trees in relation to leaf area. *Agric. Water Manage.* **49**, 65–76.

Herbst, M., Rosier, P. T., McNeil, D. D., Harding, R. J. & Gowing, D. J. 2008 Seasonal variability of interception evaporation from the canopy of a mixed deciduous forest. *Agric. For. Meteorol.* **148** (11), 1655–1667.

Herwitz, S. R. 1987 Raindrop impact and water flow on the vegetative surfaces of trees and the effects on stemflow and throughfall generation. *Earth Surf. Process. Landf.* **12**, 425–432.

Holder, C. D. 2013 Effects of leaf hydrophobicity and water droplet retention on canopy storage capacity. *Ecohydrology* **6**, 483–490.

Humbert, J. & Najjar, G. 1992 Influence de la foret sur le cycle de l'eau en domaine tempéré: Une analyse de la littérature francophone [Influence of forests on the water cycle in temperate area: An analysis of French literature]. CEREG, Louis Pasteur University, Strasbourg, France.

Janeau, J. L., Grellier, S. & Podwojewski, P. 2015 Influence of rainfall interception by endemic plants versus short cycle crops on water infiltration in high altitude ecosystems of Ecuador. *Hydrol. Res.* **46** (6), 1008–1018.

Keim, R. F. & Skaugset, A. E. 2004 A linear system model of dynamic throughfall rates beneath forest canopies. *Water Resour. Res.* **40**, 1–12.

Keim, R. F., Skaugset, A. E. & Weiler, M. 2006 Storage of water on vegetation under simulated rainfall of varying intensity. *Adv. Water Resour.* **29**, 974–986.

Kondo, J., Watanabe, T. & Nakazono, M. 1992 Estimation of forest rainfall interception (in Japanese). *Tenki* **39**, 159–167.

Levia, D. F., Michalzik, B., Näthe, K., Bischoff, S., Richter, S. & Legates, D. R. 2015 Differential stemflow yield from European beech saplings: the role of individual canopy structure metrics. *Hydrol. Process.* **29**, 43–51.

Li, X., Niu, J. & Xie, B. 2013 Study on hydrological functions of litter layers in North China. *PLoS One* **8**, 1–13.

Livesley, S. J., Baudinette, B. & Glover, D. 2014 Rainfall interception and stem flow by eucalypt street trees – The impacts of canopy density and bark type. *Urban For. Urban Green.* **13**, 192–197.

Llorens, P. & Domingo, F. 2007 Rainfall partitioning by vegetation under Mediterranean conditions. A review of studies in Europe. *J. Hydrol.* **335**, 37–54.

Moore, I. D., Hirschi, M. C. & Barfield, B. J. 1983 Kentucky rainfall simulator. *T. ASAE* **26**, 1085–1089.

Muzylo, A., Llorens, P., Valente, F., Keizer, J. J., Domingo, F. & Gash, J. H. C. 2009 A review of rainfall interception modelling. *J. Hydrol.* **370**, 191–206.

Nanko, K., Watanabeb, A., Hottac, N. & Suzuki, M. 2013 Physical interpretation of the difference in drop size distributions of leaf drips among tree species. *Agr. Forest Meteorol.* **169**, 74–84.

Pitman, J. I. 1989 Rainfall interception by Bracjen in open habitats – Relations between leaf area, canopy storage and drainage rate. *J. Hydrol.* **105**, 317–334.

Price, A. G. & Carlyle-Moses, D. E. 2003 Measurement and modelling of growing-season canopy water fluxes in a mature mixed deciduous forest stand, southern Ontario, Canada. *Agr. Forest Meteorol.* **119**, 69–85.

Pugh, E. T. & Small, E. E. 2013 The impact of beetle-induced conifer death on stand-scale canopy snow interception. *Hydrol. Res.* **44** (4), 644–657.

Rutter, A. J., Kershaw, K. A., Robins, P. C. & Morton, A. J. 1971 A predictive model of rainfall interception in forests, 1. Derivation of the model from observations in a plantation of Corsican pine. *Agric. Meteorol.* **9**, 367–384.

Safeeq, M. & Fares, A. 2014 Interception losses in three non-native Hawaiian forest stands. *Hydrol. Process.* **28**, 237–254.

Savenije, H. H. G. 2004 The importance of interception and why we should delete the term evapotranspiration from our vocabulary. *Hydrol. Process.* **18**, 1507–1511.

van Dijk, A. & Bruijnzeel, L. A. 2001a Modelling rainfall interception by vegetation of variable density using an adapted analytical model. Part 1. Model description. *J. Hydrol.* **247** (3–4), 230–238.

van Dijk, A. & Bruijnzeel, L. A. 2001b Modelling rainfall interception by vegetation of variable density using an adapted analytical model. Part 2. Model validation for a tropical upland mixed cropping system. *J. Hydrol.* **247** (3–4), 239–262.

Wang, A., Diao, Y., Pei, T., Jin, C. & Zhu, J. 2007 A semi-theoretical model of canopy rainfall interception for a broad-leaved tree. *Hydrol. Process.* **21** (18), 2458–2463.

Watson, D. J. 1947 Comparative physiological studies on the growth of field crops: variation in net assimilation rate and leaf area between species and varieties and within and between years. *Ann. Bot.* **11**, 41–76.

Wilson, T. G., Cortis, C., Montaldo, N. & Albertson, J. D. 2014 Development and testing of a large, transportable rainfall simulator for plot-scale runoff and parameter estimation. *Hydrol. Earth Syst. Sci.* **18**, 4169–4183.

Xiao, Q. F. & McPherson, E. G. 2011 Rainfall interception of three trees in Oakland, California. *Urban Ecosyst.* **14**, 755–769.

Xiao, Q. & McPherson, E. G. 2015 Surface water storage capacity of twenty tree species in Davis, California. *J. Environ. Qual.* **44**, 291–302.

Xiao, Q. F., McPherson, E. G., Ustin, S. L., Grismer, M. E. & Simpson, J. R. 2000a Winter rainfall interception by two mature open-grown trees in Davis, California. *Hydrol. Process.* **14**, 763–784.

Xiao, Q. F., McPherson, E. G., Ustin, S. L. & Grismer, M. E. 2000b A new approach to modeling tree rainfall interception. *J Geophys Res-Atmos* **105**, 29173–29188.

Zhang, G. H., Liu, B. Y. & Li, P. K. 2007 Principles and properties of artificial trough rainfall simulator. *Bul. Soil. Water Conserv.* **27** (6), 56–60 (in Chinese with English abstract).

Zhong, Y. D., Jia, Y. W. & Li, Z. W. 2013 Spatial and temporal changes of maximum 1 h precipitation intensity in Beijing region in last 53 years. *J. China Hydrol.* **33**, 32–37 (in Chinese with English Abstract).

First received 31 March 2015; accepted in revised form 28 September 2015. Available online 13 November 2015